P148

IDEALIZED SIMULATIONS OF MERGERS BETWEEN SQUALL LINES AND ISOLATED SUPERCELL THUNDERSTORMS

Adam J. French*
South Dakota School of Mines and Technology, Rapid City, South Dakota
Matthew D. Parker
North Carolina State University, Raleigh, North Carolina

1. INTRODUCTION AND BACKGROUND

Mergers between quasi linear convective systems (squall lines) and isolated supercells pose a challenge to warning forecasters as the changes in storm organization that result from the merger can present an evolving severe weather threat. Past studies have examined such merger events as a potential instigator for tornadogenesis, with a number of studies documenting cases where squall line-supercell mergers appear to coincide with the development of tornadoes (e.g., Goodman and Knupp 1993; Sabones et al. 1996; Wolf et al. 1996; Wolf 1998). More recently French and Parker (2012) documented an evolving severe weather threat in an analysis of 22 observed cases of these types of mergers. Generally speaking, any strong, long-lived tornadoes and large hail occurred with the isolated supercells prior to the merger, while severe straight-line wind reports were maximized post-merger. Furthermore, the mergers were observed to precede several key changes in storm structure. In most cases the merged system evolved into one of three patterns of bow echo organization (French and Parker 2012, their fig. 7) and a post-merger increase in low-level storm rotation following the merger was also commonly observed (French and Parker 2012, their figs. 11 and 14).

This past work demonstrates that squall line-supercell mergers can have important implications for storm morphology and, as a result, severe weather production. However, the observations used in these studies have been of insufficient to determine the key processes that drive these observed changes. As a result, the present study has used an idealized numerical simulation of a squall line-supercell merger to examine the storm-scale processes at work in these events. Our ultimate goal is to develop a conceptual model to explain the dynamical processes responsible for the behavior observed when a squall line merges with an isolated supercell.

2. METHODS

This work utilized 3D idealized numerical model simulations using version 1.16 of the Bryan cloud model (CM1) described by Bryan and Fritsch (2002). We used a horizontal grid spacing of 500 m as a compromise in order to sufficiently resolve convective-scale processes while also keeping computing costs manageable given the 300 x 400 x 20 km grid necessary to simulate a squall line, supercell and merged system. The vertical grid spacing was stretched from 100 m at the surface to 250 m above z=2500 m. We employed open x- and y- lateral boundary conditions, free-slip upper and lower boundary conditions, and a Rayleigh damping layer above 14 km. In the interest of keeping these simulations as simple as possible radiative effects, surface friction and surface fluxes were all neglected. The simulations do include Coriolis forcing, applied to perturbation values only at a constant value of $f = 1 \times 10^{-4}\text{s}^{-1}$ across the entire domain (i.e. an f-plane). This was included because initial tests revealed that it was necessary in order to produce the asymmetric structures (i.e. a dominant cyclonic line-end vortex at the north end of the squall line) similar to what was observed for real-world mergers. This is not surprising as the convergence of planetary vorticity has been shown by a number of studies to be important to the development of cyclonic mesoscale vortices over a wide range of scales (i.e. Skamarock et al. 1994; Weisman 1993; Atkins and St. Laurent 2009). The present simulations used a horizontally homogeneous background environment (Fig. 1a), based on the idealized environment of Weisman and Klemp (1982), which has been widely used in the simulation of convective storms. The squall line was triggered using a 200 km long (y-dimension), 10 km wide, 3 km deep line thermal with a potential temperature perturbation of +2 K. Random noise of +/− 0.1 K was added to the thermal to help develop 3 dimensional structures along the line. A supercell was triggered 3 hours into the simulation using a single warm bubble

**Corresponding author address:* Adam J. French, Department of Atmospheric Sciences, South Dakota School of Mines and Technology, 501 E. St. Joseph St., Rapid City, SD 57701. E-mail: adam.french@sdsmt.edu

positioned approximately 60 km ahead of the developing squall line.

Experience revealed that the main challenge in simulating a squall line-supercell merger lies with producing both convective modes simultaneously within a single simulation. In many cases a simulation that produced a reasonable supercell storm would not produce an effective squall line, and vice-versa. To address this issue, we employed the "base-state substitution" BSS technique discussed in detail by Letkewicz et al. (2012, manuscript submitted to *Mon. Wea. Rev.*) to employ two different wind profiles throughout the simulation in order to control storm organization (Fig. 2). First, we initiated a squall line in an environment characterized by a favorable, unidirectional wind profile (Fig. 1a) and let it mature for three hours, essentially the time it took for the line to become steady. At this point, we wrote a restart file containing all of the run-time model fields, and modified the base-state wind profile within the restart file to resemble one more characteristic of a supercell environment, namely moderate (25 m s^{-1}) deep-layer shear and a low-level shear vector that veers with height (Fig. 1b).

As illustrated in figure 2, this was done by separating the original base-state wind profile from the perturbations that had developed in the course of running the 3-hour squall line simulation, introducing the new base-state wind profile, and then adding the original storm-induced perturbations back on to the new wind profile. In doing this we are able create a more favorable environment for supercells, while still maintaining the physical perturbations to the wind and thermodynamic fields produced by the squall line. The base state thermodynamic profile is left untouched; the small changes in values of CAPE and CIN between Figs. 1a and b are perturbations solely due to the presence of the squall line. Once the modifications are complete, we restart the simulation using the modified restart file, and trigger the supercell ahead of the squall line with a warm bubble.

This paper will focus on the results of two simulations run using this method. The includes a supercell triggered ahead of the line following the restart (hereafter the "MERGER" simulation) allowing us to simulate a squall line supercell merger. The second includes the change in the wind profile, but without the supercell being triggered (hereafter the "NOMERGER" simulation) to assess how a squall line would evolve in the higher-shear environment absent the merger.

3. RESULTS

3.1 Overview of idealized merger simulation

We will begin our discussion with an overview comparing the MERGER and NOMERGER simulations. The squall lines in the MERGER and NOMERGER simulations evolve nearly identically until just before the onset of the merger with the supercell. At this point, in the MERGER simulation, the squall line begins to weaken in the vicinity of the supercell, evident as a decline in simulated radar reflectivity in figure 3a-b. As the merger progresses, the supercell becomes the new northern end of the squall line, and an increase in simulated radar reflectivity is seen to the south of the merged supercell (Fig. 3c-d). This region ultimately accelerates eastward, producing a pronounced, but compact bow echo to the south of the remnant supercell (Fig. 3e-f). The period immediately following the merger is also characterized by an increase in low-level vertical vorticity. As the merger begins, there is a rapid increase in vertical vorticity within the lowest 1 km AGL in the simulation (colored shading, Fig 3). Over time, this area expands, eventually developing into a broad area of primarily cyclonic vorticity located north of the developing bow echo, characteristic of a cyclonic line-end vortex that is common to the bow echo organization (e.g. Weisman 1993). Finally, shortly after the merger, a strong rear inflow jet begins to appear in the lowest few kilometers above ground, and likely plays a role in the development of the bow echo (blue vectors, Fig 3). Many of these features, particularly the simulated radar evolution and development of strong low-level vertical vorticity are consistent with structures identified in observed squall line-supercell merger cases by French and Parker 2012. This gives us confidence that our simulations effectively capture this phenomenon.

Comparing the MERGER simulation to the NOMERGER simulation, we find that even without the merging supercell the squall line evolves into a bow echo (Fig. 4a-f). This is not surprising given that the strong vertical shear profile added following the BSS should favor bow echo organization (e.g. Weisman 1993; Evans and Doswell 2001). However, while similar in terms of gross storm morphology, the details of the bowing in the two simulations are quite different. The NOMERGER simulation produces a very broad bow, encompassing most of the squall line, and the bow begins to emerge by approximately 275 minutes into the simulation (Fig. 4b). Meanwhile the MERGER simulation produces a bow that is much more compact in north-south extent, while also appearing more pronounced (i.e. more concave), and does not fully develop until approximately 310 minutes into the simulation (Fig. 3e). Furthermore, the NOMERGER simulation does not produce the strong low-level vertical vorticity seen in the MERGER simulation, nor does it appear to produce as many squall line mesovortices. Thus, while the background environment favors development of a bow echo, the merger plays an important role in modulating the details, intensity, and timing of the bowing, not to mention the development of low-level storm rotation. We will next take an in-depth look at several of the key processes responsible for the simulated post-merger evolution.

3.2 Cold pool evolution

One aspect of the early merger evolution that is of particular interest is the weakening of the squall line in the vicinity of the merger, evident in both the present simulations as well as an many observed cases. An analysis of the surface potential temperature field (not shown) reveals that the decline in squall line intensity begins approximately the same time that outflow from the isolated supercell begins to reach the squall line's gust front. The nature of this interaction is illustrated by examining the low level potential temperature gradient associated with the squall line's gust front (Fig. 5a-e). As the outflow from the supercell reaches the gust front (Fig. 5b), the potential temperature gradient rapidly weakens, becoming non-existent within 20 minutes of the first interaction (Fig. 5c-e).

The result of this weakening is twofold. First, since the speed of the gust front can be approximated by the speed of a density current, it is proportional to the strength of the density gradient across the gust front. As this gradient weakens, the forward motion of the gust front stalls. This keeps the gust front from overtaking the supercell. Secondly, the strength of lifting along the gust front is also driven in part by the strength of the gust front density gradient. As this gradient weakens, so too does the low-level lifting along the gust front that is sustaining the squall line, vanishing completely by 140 minutes into the simulation (Fig. 5f-j).

The ultimate result of the stalling of the gust front, and subsequent removal of gust front lifting is that the portion of the squall line involved in the merger weakens and the supercell becomes the new leading edge of the squall line. This leads to the supercell playing a dominant role in the post-merger evolution, rather than being overwhelmed or "absorbed" by the squall line. This finding meshes well with observations of areas of weak radar reflectivity preceding the merger by French and Parker (2012) and of a "distortion" of the squall line's just front in the merger case observed by Goodman and Knupp (1993).

3.3 Low-level vorticity evolution

A second feature of interest in common to observed cases, as well as the present MERGER simulation is the development of a region of strong low-level vertical vorticity associated with the merged supercell. As is clear from figures 6-9, the evolution of vertical vorticity in the MERGER simulation is quite complicated, as there are multiple vortices spanning multiple scales present before, during and after the merger. These include the mesocyclone associated with the supercell, a shallow, small-scale vortex that develops along the supercell's rear-flank gust front, several mesovortices that develop along the gust front of the squall line and later the merged system, and finally, a large line-end vortex that develops at the northern edge of the merged system as it evolves into a bow echo. A detailed analysis of the spectrum of vortices produced, and how they relate to the merger is underway, however the present discussion will focus on a low-level circulation that develops out of the remnant supercell mesocyclone as it moves rearward with respect to the merged system's gust front.

The vortex of interest originates approximately 1 km AGL near the mesocyclone of the pre-merger supercell prior to the onset of merging (Fig. 6b, red arrow). It appears to be the last in a series of cyclic episodes of low-level mesocyclogenesis that occur while the supercell is isolated. The vortex rapidly deepens, extending to approximately 5 km AGL, as was observed with earlier circulations associated with the supercell (Fig. 7). However, as this vortex moves rearward, it begins to weaken in the mid-levels (e.g. approximately 5 km AGL), while remaining strong and growing in diameter between 1 - 3 km AGL (Fig. 8). Eventually, once the vortex is well to the rear of the merged system's gust front, it begins to lower with time (Fig. 7, t=275-285 min), leading to the rapid spin-up of a region of very strong vertical vorticity at the lowest model level (Fig. 7, t=285-290 min and Fig. 9a). While the 500 m horizontal grid spacing is insufficient to resolve tornado-scale vortices, the presence of strong, concentrated, vertical vorticity at the lowest model level does suggest the potential for a tornado-like vortex. This is significant given observations in past studies of tornadoes occurring during or just after a squall line-supercell merger occurs (Goodman and Knupp

1993; Sabones et al. 1996; Wolf et al. 1996; Wolf 1998). Furthermore, this apparent descent of strong vertical vorticity is consistent with observation of strong rotation becoming concentrated in low-levels post-merger in a number of the cases examined by French and Parker (2012).

While a more quantitative analysis will be forthcoming in a future paper, we have some preliminary thoughts on the processes responsible for the development of this near-surface vortex. First, as shown in figure 9, the near-surface vortex develops in a region of strong low-level vertical wind shear (c.f. the sizable difference in wind speed and direction between the lowest model level and 1 km in Fig. 9a, b) which, by definition implies strong horizontal vorticity. This strong vertical wind shear appears to be the result of high-momentum air from the squall line's rear inflow jet (RIJ) being forced to the surface by the rear flank downdraft (RFD) of the merging supercell (note the low-level divergence signature of the RFD in Figs. 6-9). Secondly, as shown in figure 7 the descent of strong vorticity to the lowest model level is preceded by the extension of strong upward vertical velocities to this level as well. This coupled with observations that the strong core of vertical vorticity is co-located with a low-level updraft maximum leads us to speculate that updraft-tilting of horizontal vorticity and subsequent stretching of the resultant vertical vorticity may be an important driver for the development of this vortex. Thus we propose that as the remnant mesocyclone moves rearward, it feeds on the horizontal vorticity created by this strong vertical shear, which intensifies the circulation and leads to the development of the near-surface vortex. This may explain why the low-level vortex develops and persists well to the rear of the maximum buoyancy gradient along the gust front, where one would expect a maximum in baroclinically-generated horizontal vorticity to be found.

This process implies that the development of this near-surface vortex is tied directly to the squall line-supercell merger. The merger first produces a region of strong horizontal vorticity in the lowest model levels via the supercell's RFD forcing high-momentum squall line RIJ air to the surface. Then, as the remnant supercell updraft and mesocyclone encounter this strong low-level shear, they provide a mechanism to tilt this horizontal vorticity into the vertical and intensify the resultant vertical vorticity via stretching, resulting in an intense low-level vortex. We plan to quantify the details of this process more completely and present the results in a future manuscript.

3.4 Rear inflow jet and bow echo development

One of the remaining questions to emerge from the observation-based study was what role the merger itself played in producing the bow echoes that were frequently observed. Since many cases occurred in what could be classified as bow echo environments it was unclear whether the merger was a key part of bow echo development, or if the convective line would have eventually produced bow echo structures without a merger. In comparing the MERGER and NOMERGER simulations above, it is clear that both simulations produce bow echoes, suggesting, as expected, that the environment is playing an important role here. However, it is also clear that the characteristics of the bowing vary between the simulations. We will now examine how the merger may influence bow echo development in terms of the processes responsible for bow echo formation, namely the development of a strong rear inflow jet.

As shown in figure 3b-d, the merger eventually leads to a local increase in convective intensity along the squall line, which produces stronger mid-level warming than is seen in the NOMERGER simulation (Fig. 10b, d). This strong heating serves to produce a minimum buoyant pressure perturbation near the leading edge of the squall line (Fig. 10a, b), which has long been known to be a key element in producing a rear inflow jet (RIJ, e.g. Weisman 1992). This works to re-invigorate the RIJ in the MERGER simulation leading to the bowing structure observed. In comparing the MERGER and NOMERGER simulations, it is clear that the MERGER run produces a lower minimum pressure, that is more compact and displaced further south compared to the NOMERGER run (Fig. 10b, d). This explains why the strongest RIJ in the MERGER run is more compact in the north-south direction and located further south than in the NOMERGER run (Fig. 10a, c), consistent with differences in the location and scale of the bowing between the two runs. At the time shown, the RIJ in the MERGER simulation is still re-developing after weakening prior to the merger (e.g. when the squall line initially weakened),leading to wind speeds that are comparable to the NOMERGER run despite lower minimum pressure perturbation. This demonstrates that while the environment favors bowing with or without a merger, the merger plays an important role in modulating the storm scale characteristics of the bow, including its size, location and intensity.

4. CONCLUSIONS AND FUTURE WORK

Idealized simulations have been run that capture the salient features of observed squall line-supercell merger cases, revealing some of the key processes at work. Specifically:

1. The merger is preceded by a weakening of the squall lines cold pool, leading to a local decline in squall line intensity. This results in the supercell being preserved during the merger and playing a dominant role in the merged system.
2. Following the merger, an increase in low-level vorticity is observed to the rear of the merged system's gust front, associated with the remnant supercell mesocyclone. This vortex appears to develop due to the tilting of horizontal vorticity that results from strong vertical wind shear following the descent of the rear-inflow jet.
3. The merger produces an increase in convective intensity, producing strong warming aloft. This generates a local minimum in perturbation pressure near the leading edge of the merged system, driving a re-intensification of the squall line's rear inflow jet that leads to post-merger bow echo development.

Additionally, comparisons between a simulation run with the merger included (MERGER) and one without the merger supercell (NOMERGER) reveal that while bow echoes are present in both simulations, the merger has a significant impact on the nature of the bowing that results. As one might expect, this has important effects for the sensible weather associated with the merged system, as the MERGER run produces 1) stronger surface winds; 2) larger near-surface vertical vorticity; and 3) heavier rainfall in the vicinity of the merger (Fig. 11). These results are largely consistent with observations of merger events, both in terms of storm structure as well as with the merger producing severe weather in many cases. However, the simulations also imply that the merger itself may provide a region of particularly severe weather along the squall line, a finding that could not be determined from severe weather reports alone due to the lack of accurate null reports along the squall line, away from the merger.

The present study has focused on the stormscale dynamic processes involved in squall line supercell mergers. Future work is planned to attempt to address the question as to why a range of bow echo structures are observed in these cases (e.g. French and Parker 2012) using a series of idealized experiments to test different background environments, merger locations, storm motions and forcing mechanisms.

ACKNOWLEDGMENTS We would like to thank George Bryan for developing and maintaining the model used to run these simulations (CM1) and making it freely available. Computational and data storage resources for initial simulations were provided by the Office of Information Technology High Performance Computing at North Carolina State University and Renaissance Computing Institute. This research has been supported by NSF grants ATM-0552154 and ATM-0758509.

References

Atkins, N. T. and M. St. Laurent, 2009: Bow echo mesovortices: Part II: Their genesis. *Mon. Wea. Rev.*, **137**, 1514–1532.

Bryan, G. H. and M. J. Fritsch, 2002: A benchmark simulation for moist nonhydrostatic numerical models. *Mon. Wea. Rev.*, **128**, 3941–3961.

Evans, J. S. and C. A. Doswell, 2001: Examination of derecho environments using proximity soundings. *Wea. Forecasting*, **16**, 329–342.

French, A. J. and M. D. Parker, 2012: Observations of mergers between squall lines and isolated supercell thunderstorms. *Wea. Forecasting*, **27**, 255–278.

Goodman, S. J. and K. R. Knupp, 1993, Tornadogenesis via squall line and supercell interaction: The November 15, 1989, Huntsville, Alabama, tornado. *The Tornado: Its Structure, Dynamics, Prediction, and Hazards*. No. 79, Amer. Geophys. Union.

Sabones, M., E. M. Agee, and M. Akridge, 1996, The Pulaski county and West Lafayette, Indiana tornadoes, 26-27 April 1994: A case of supercell (mesocyclone) and squall line bow-echo interaction. Preprints, *18th Conf. Severe Local Storms*, San Francisco, CA, Amer. Meteor. Soc.

Skamarock, W. C., M. L. Weisman, and J. B. Klemp, 1994: Three-dimensional evolution of simulated long-lived sqaull lines. *J. Atmos. Sci.*, **51**, 2563–2584.

Weisman, M. L., 1992: The role of convectively generated rear–inflow jets in the evolution of long–lived mesoconvective systems. *J. Atmos. Sci.*, **49**, 1826–1847.

———, 1993: The genesis of severe, long–lived bow echoes. *J. Atmos. Sci.*, **50**, 645–670.

Weisman, M. L. and J. B. Klemp, 1982: The dependence of numerically simulated convective storms on vertical wind shear and buoyancy. *Mon. Wea. Rev.*, **110**, 504–520.

Wolf, P. L., 1998: WSR-88D radar depiction of supercell-bow echo interaction: Unexpected evolution of a large, tornadic "comma-shaped" supercell over eastern Oklahoma. *Wea. Forecasting*, **13**, 492–504.

Wolf, R., R. Przybylinski, and P. Berg, 1996, Observations of a merging bowing segment and supercell. Preprints, *18th Conf. Severe Local Storms*, San Francisco, CA, Amer. Meteor. Soc.

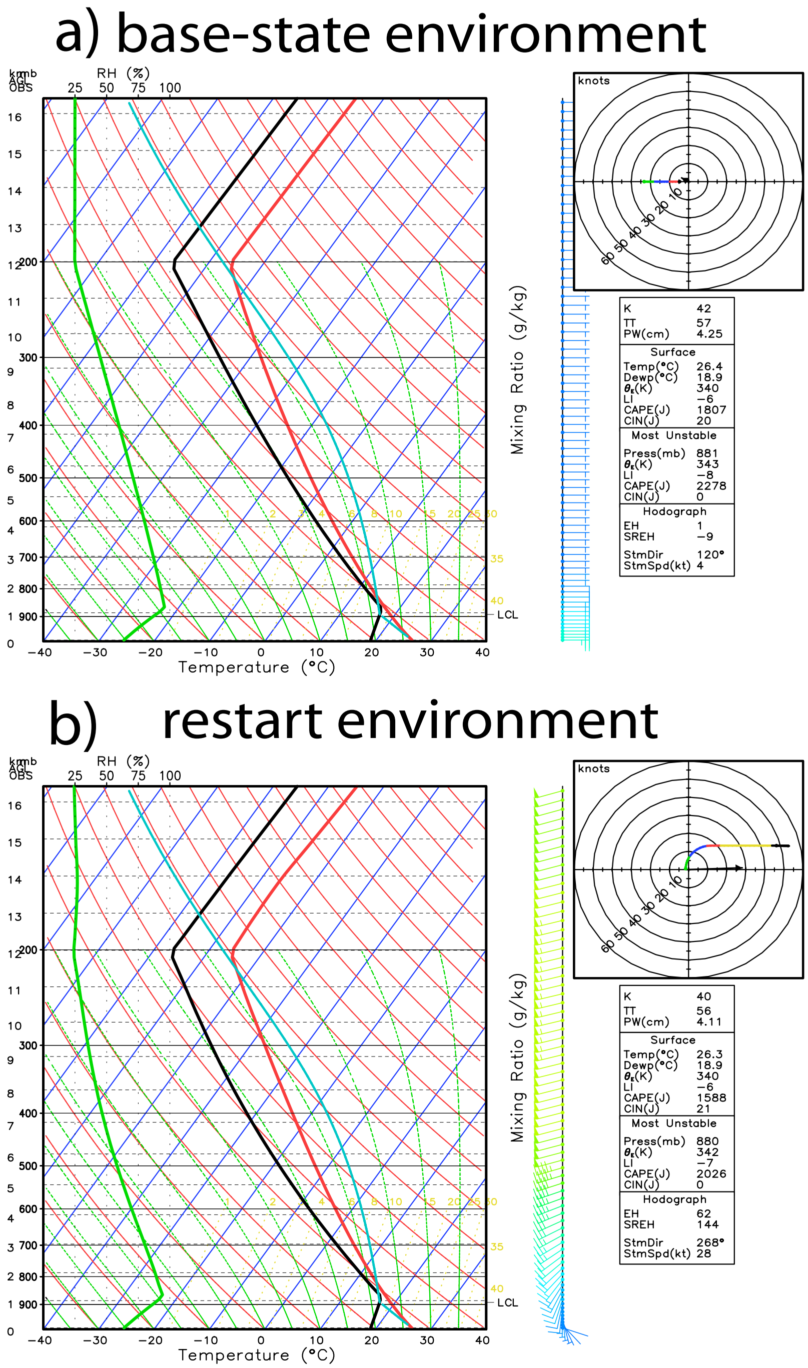

Figure 1: Skew-T log-P diagrams and hodographs depicting the horizontally homogeneous background environments for (a) the initial 2-hours of simulation time and (b) the stronger vertical shear environment introduced two hours into the simulation (after the BSS)

.

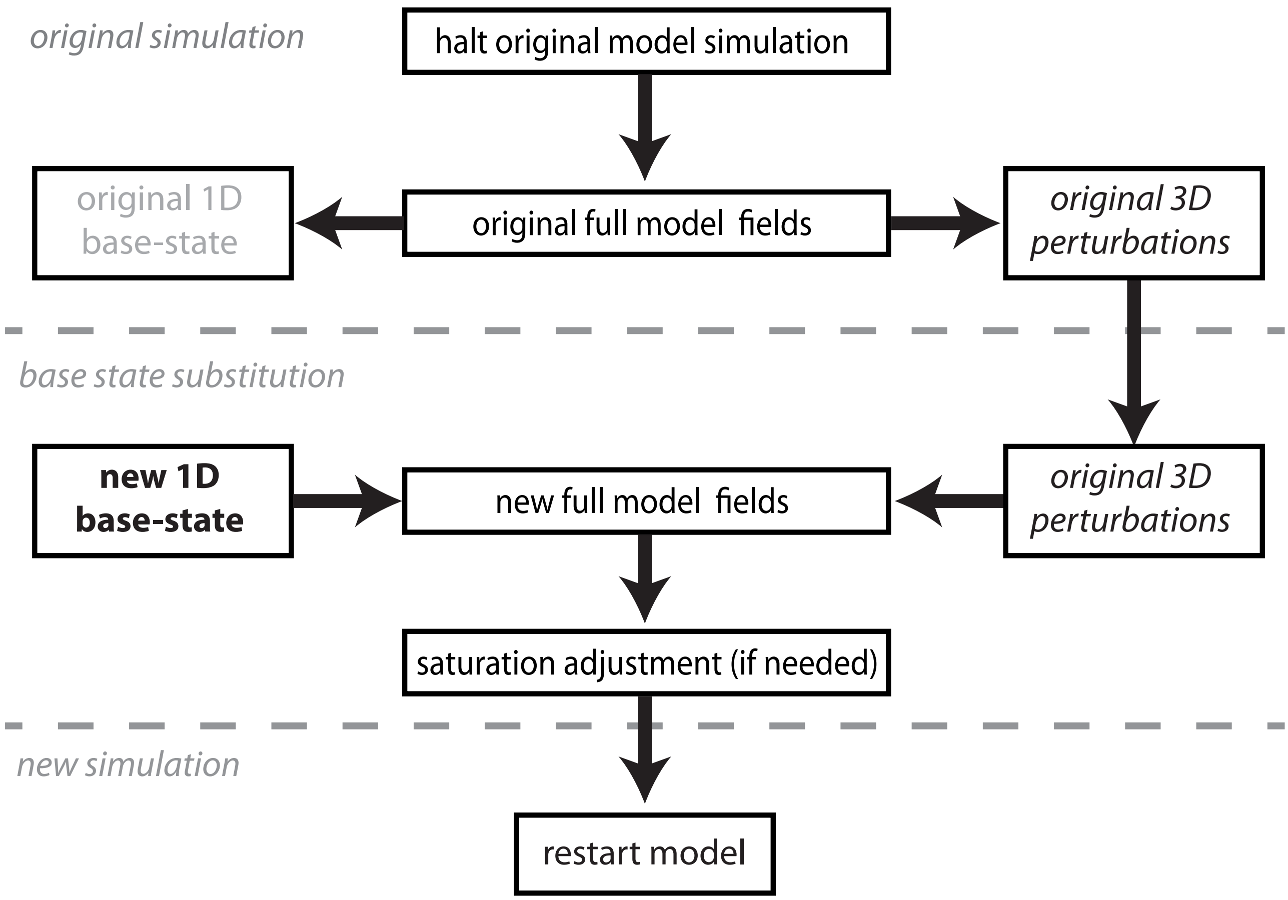

Figure 2: Schematic diagram illustrating the Base State Substitution method used to replace the background wind profile 2 hours into the simulations.

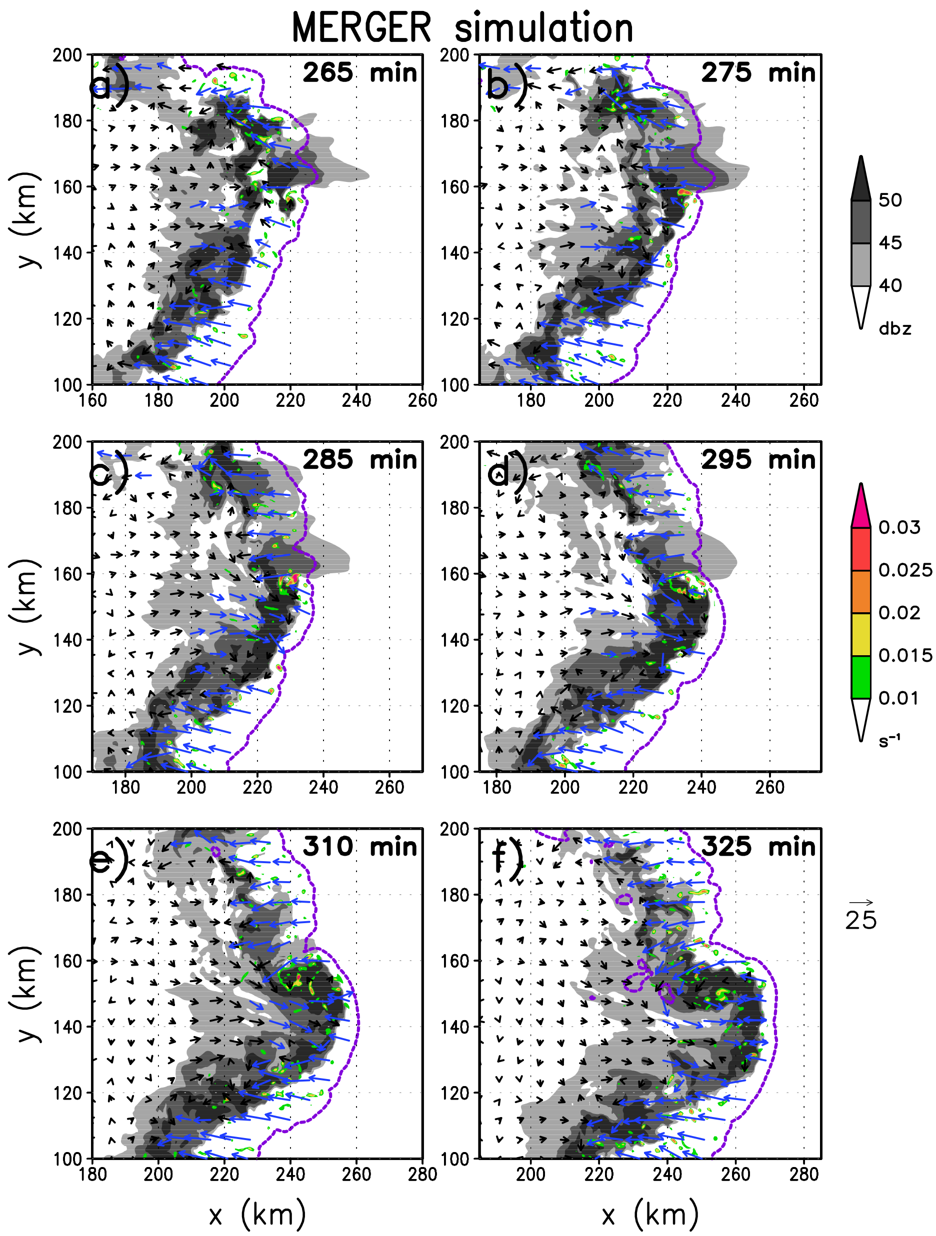

Figure 3: Summary plot of simulated radar reflectivity (dBZ, grey shading), vertical vorticity (s^{-1}, positive values shaded in color), $-2K$ potential temperature perturbation (dashed purple contour), and 1 km AGL storm-relative wind vectors within the storm (blue vectors > 20 m s^{-1}) at (a) 265, (b) 275, (c) 285, (d) 295, (e) 310, and (f) 325 min. into the MERGER simulation.

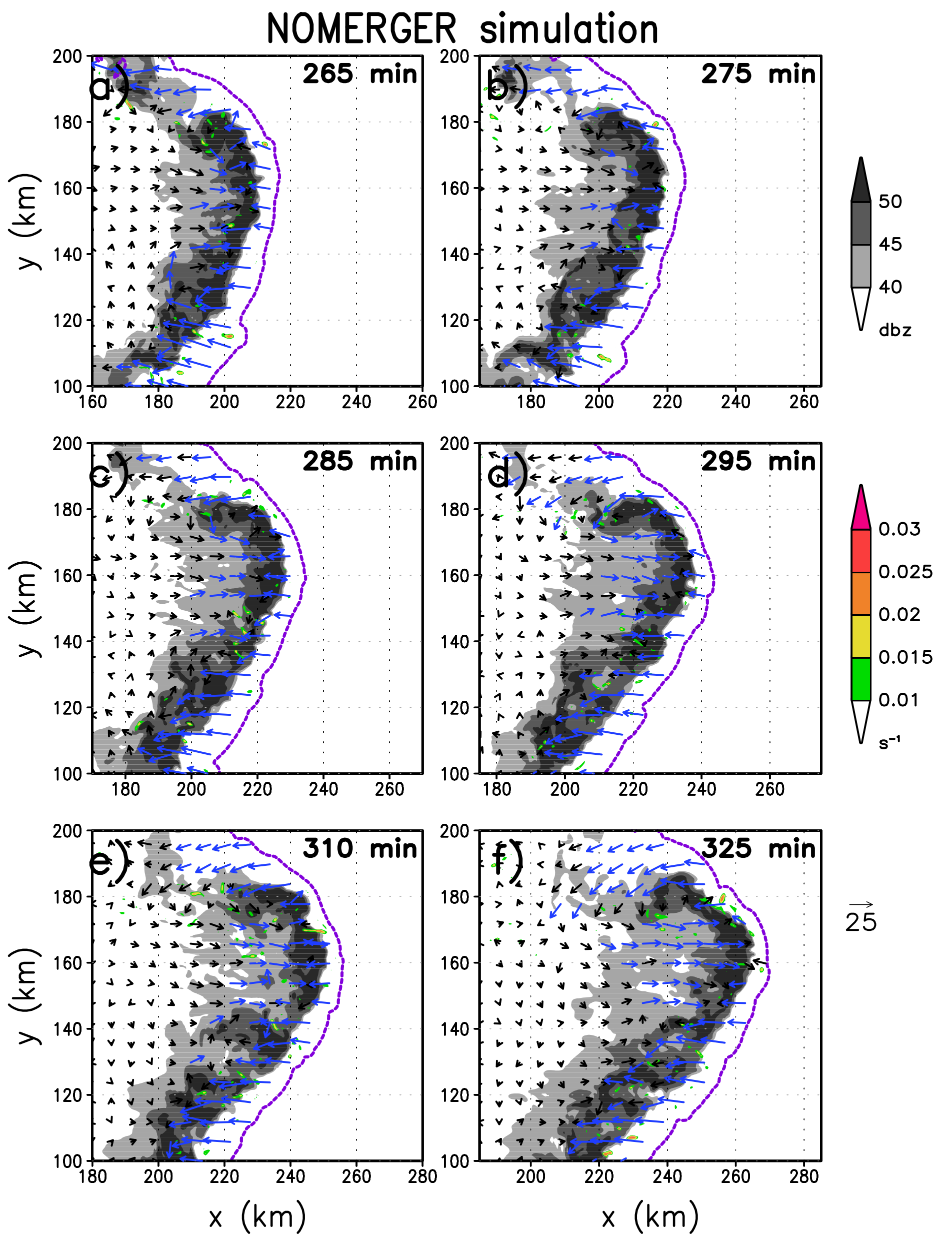

Figure 4: As in Fig. 3, but for NOMERGER simulation.

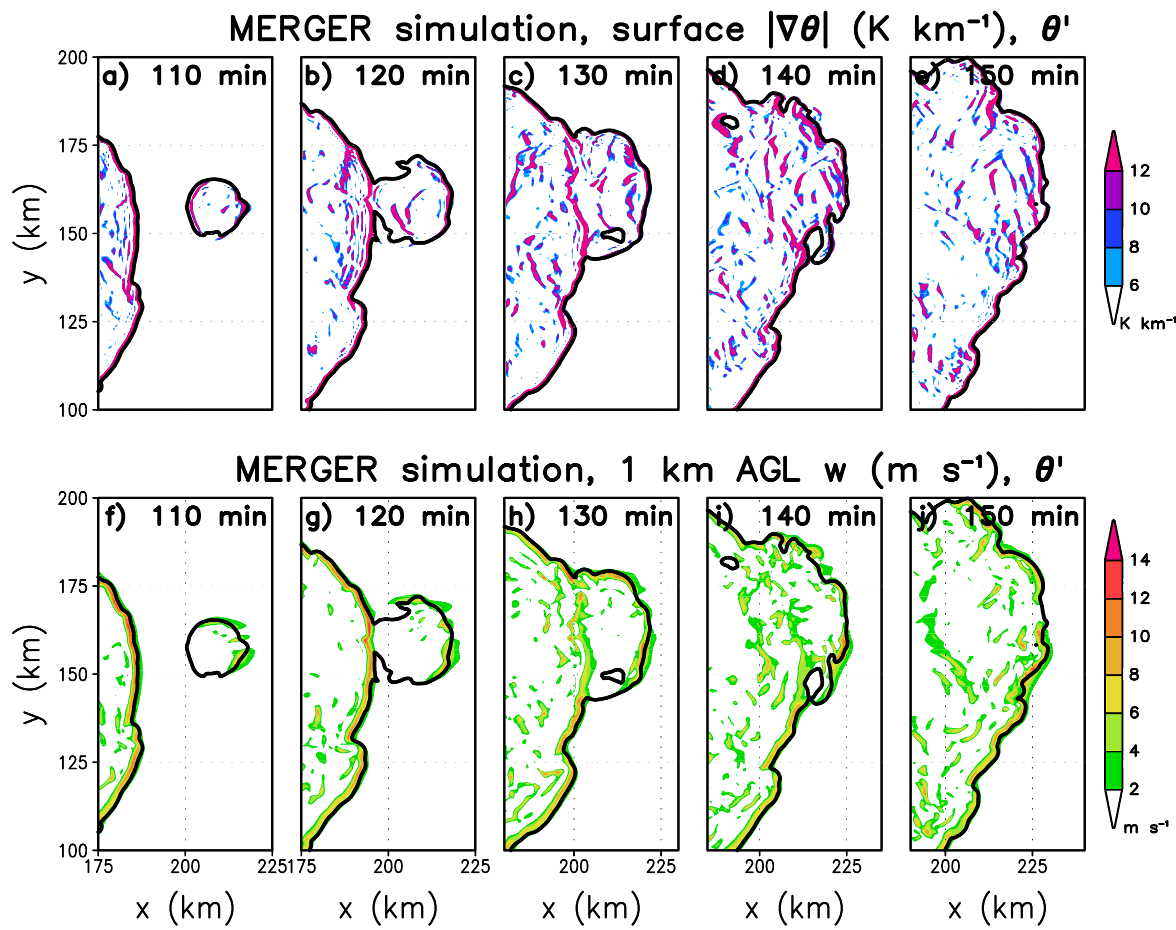

Figure 5: (a-e) Magnitude of the surface potential temperature gradient (K km^{-1}, shaded as shown) and -2 K potential temperature contour (black contour) and (f-j) 1 km AGL vertical velocity (m s^{-1}, shaded as shown) and -2 K potential temperature contour (black contour) between 110 and 150 minutes into the MERGER simulation.

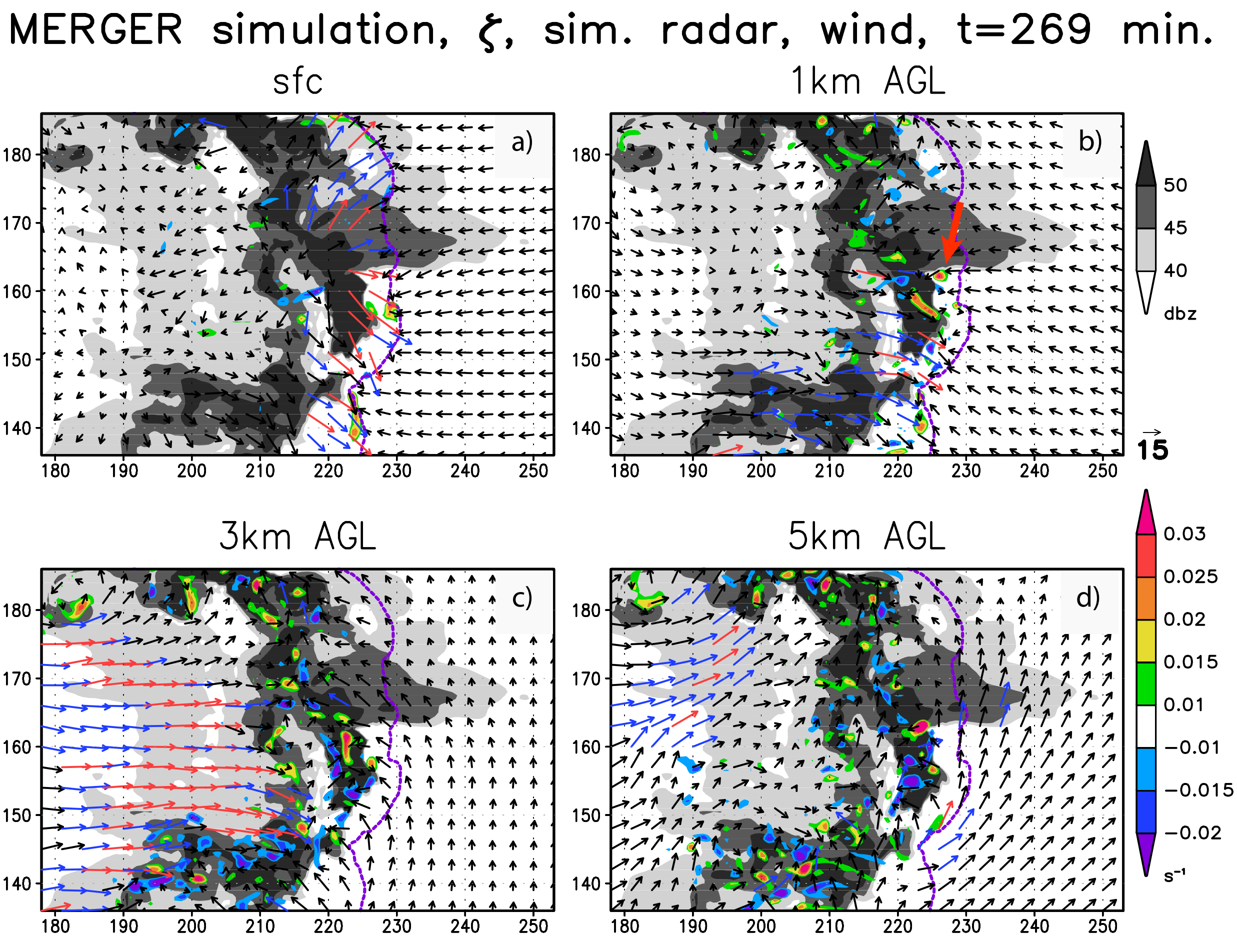

Figure 6: Simulated radar reflectivity at 1 km AGL (dBz, gray shading), -2 K surface potential temperature perturbation (purple contour), and vertical vorticity (s^{-1}, colored shading, and ground-relative wind vectors (blue $>$ 20 m s^{-1}, red $>$ 25 m s^{-1}) at a) the lowest model level, b) 1 km AGL, c) 3 km AGL, and d) 5 km AGL at 269 minutes into the MERGER simulation.

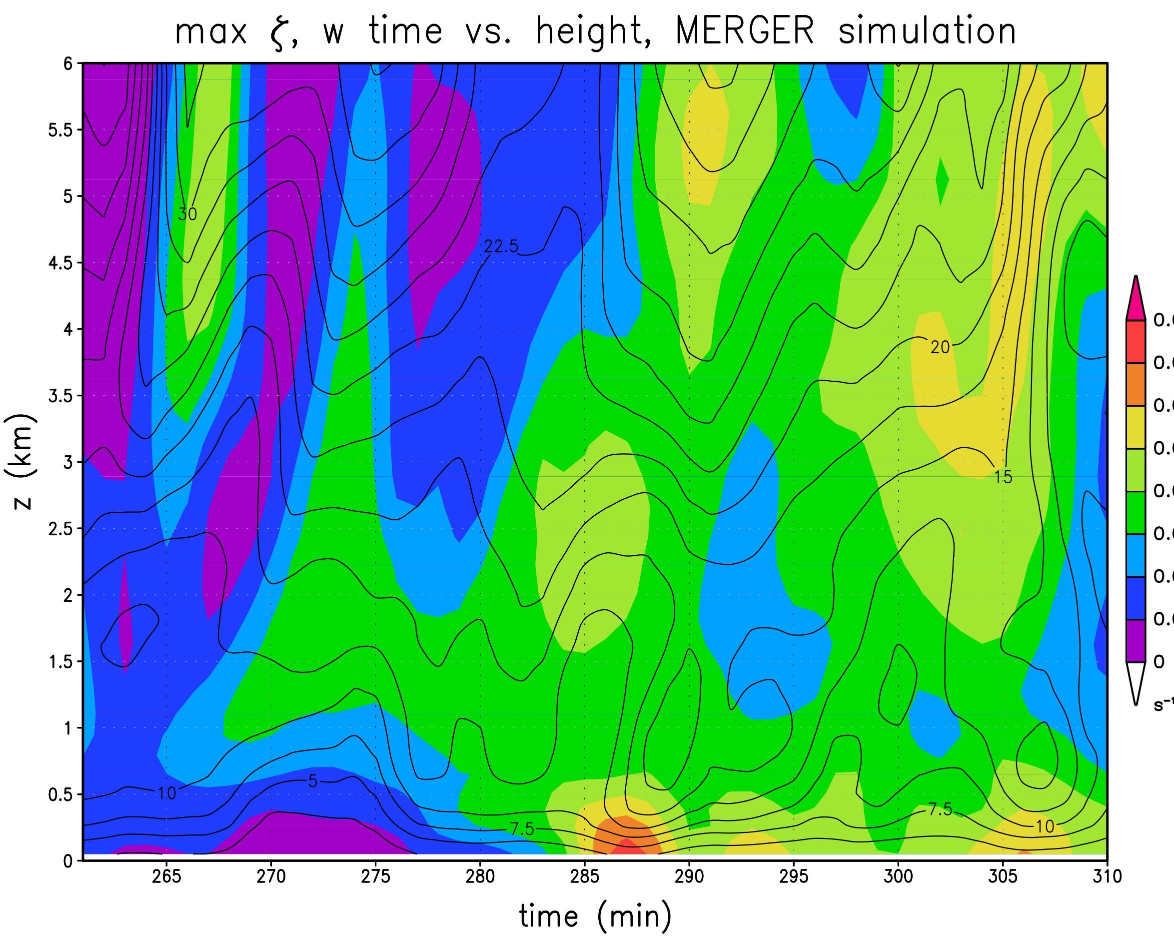

Figure 7: Time vs. height plot of maximum vertical vorticity and maximum vertical velocity associated with the circulation discussed in the text.

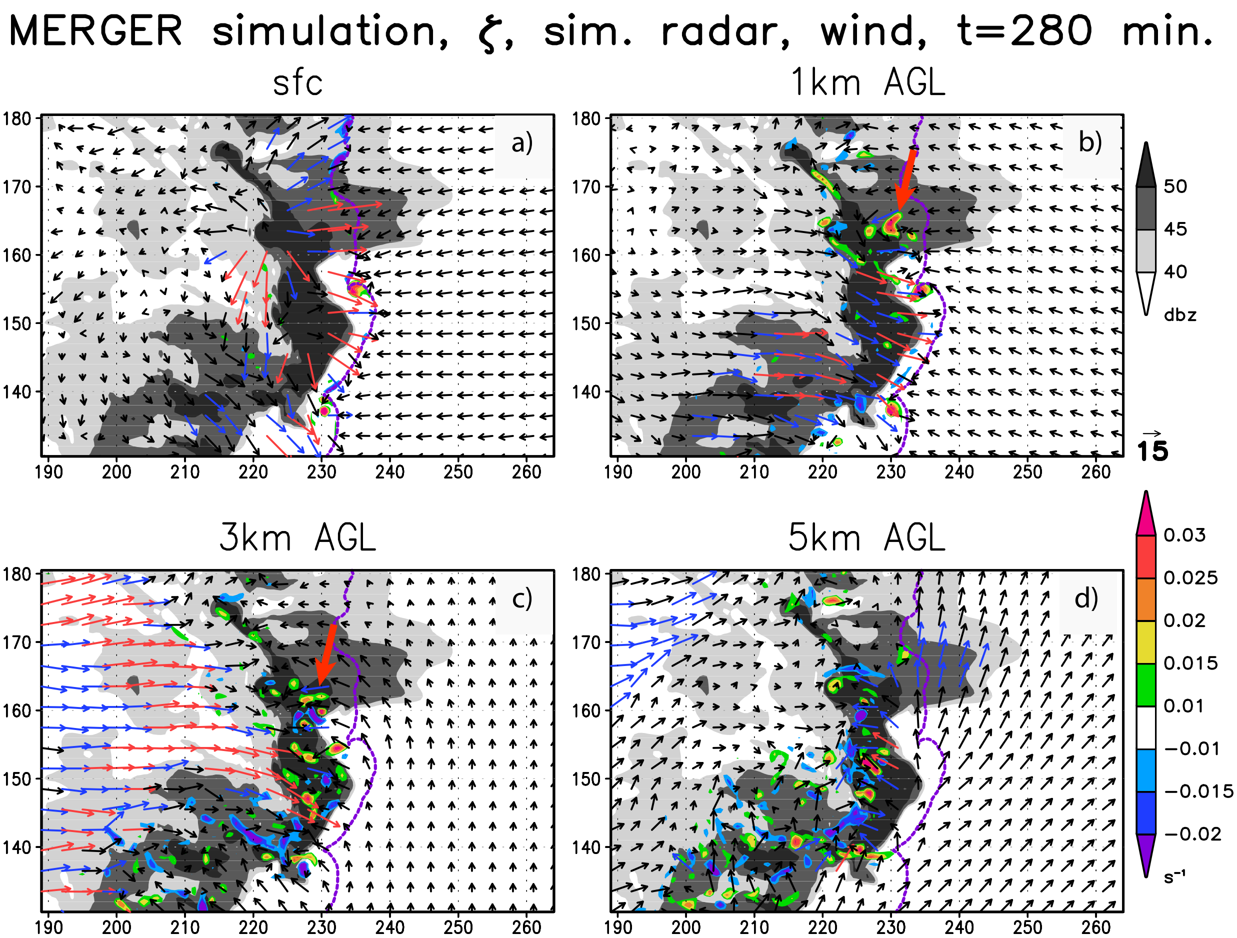

Figure 8: As in Fig. 6, but at 269 minutes into the MERGER simulation.

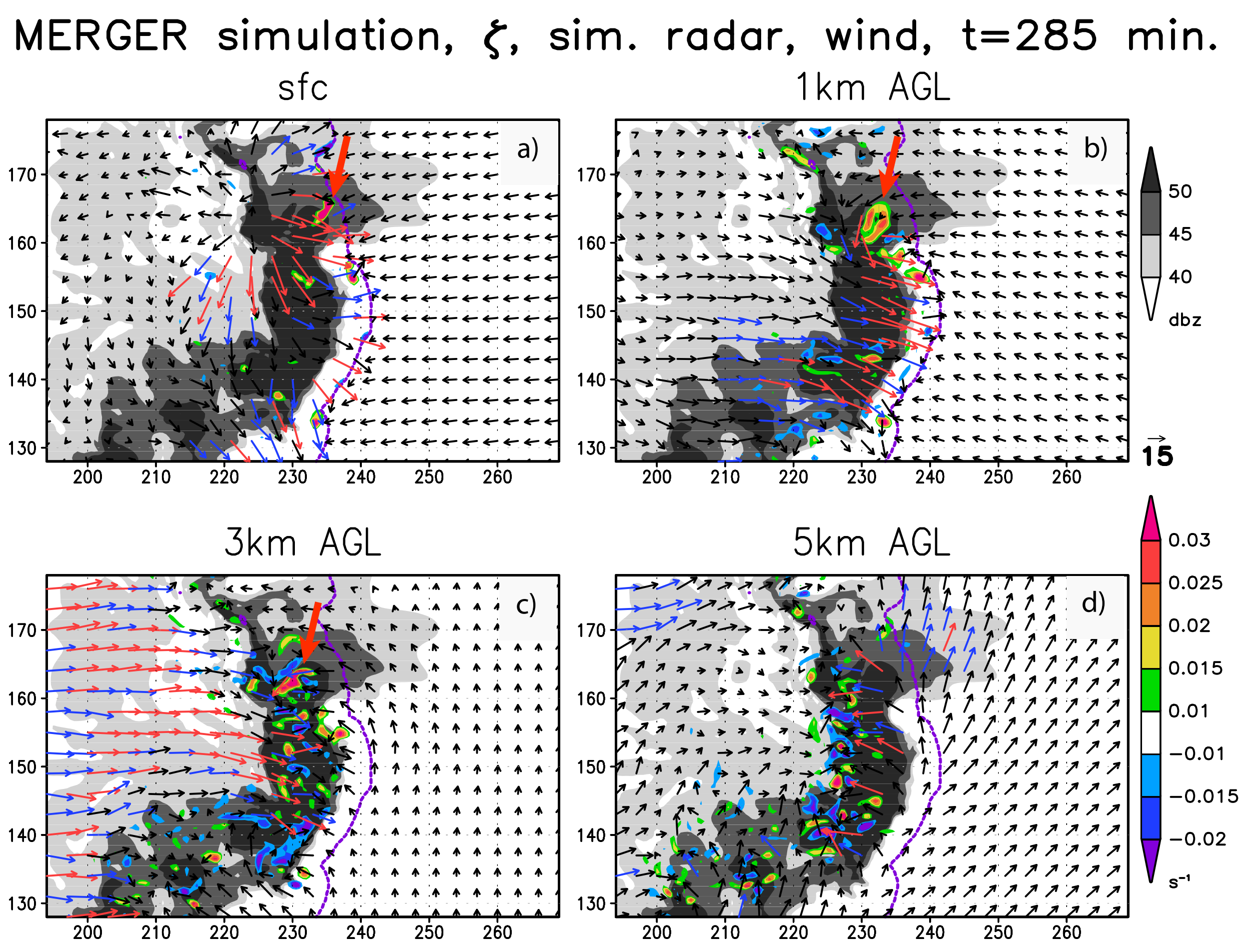

Figure 9: As in Fig. 6, but at 269 minutes into the MERGER simulation.

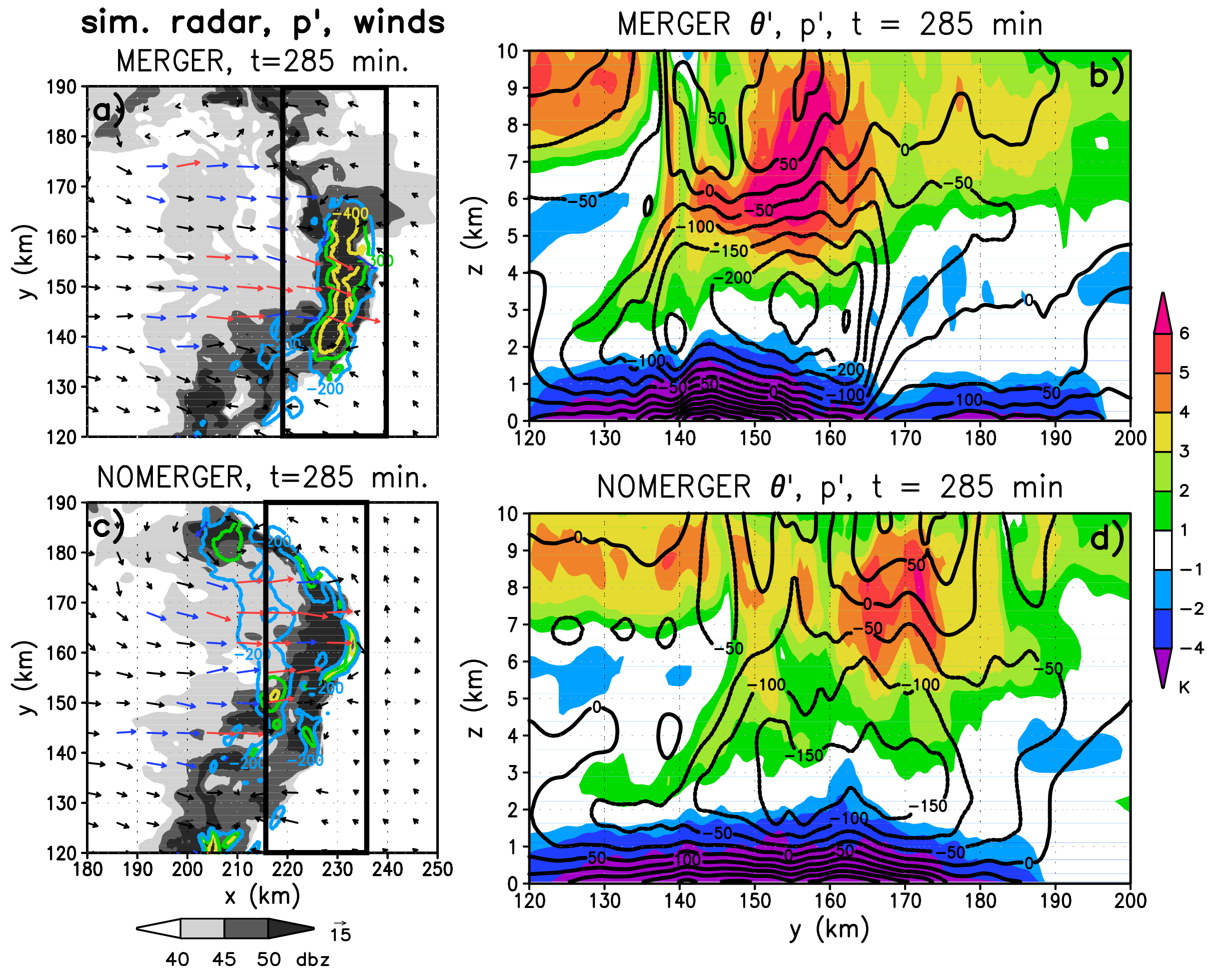

Figure 10: Left panels: Plan view of simulated radar reflectivity (dBZ, gray shading), ground relative wind vectors (m s^{-1}, vectors > 20 and 25 m s^{-1} shaded blue and red, respectively), and pressure perturbation averaged between 1 and 2 km AGL (Pa, colored contours). Right panels: Cross section of potential temperature perturbation (K, shaded as shown) and pressure perturbation (Pa, black contours) averaged in the x-direction over the box shown in a, and c. Top panels (a,b) are from the MERGER simulation and bottom panels (c, d) are from the NOMERGER simulation. All plots are at 285 minutes into the respective simulations.

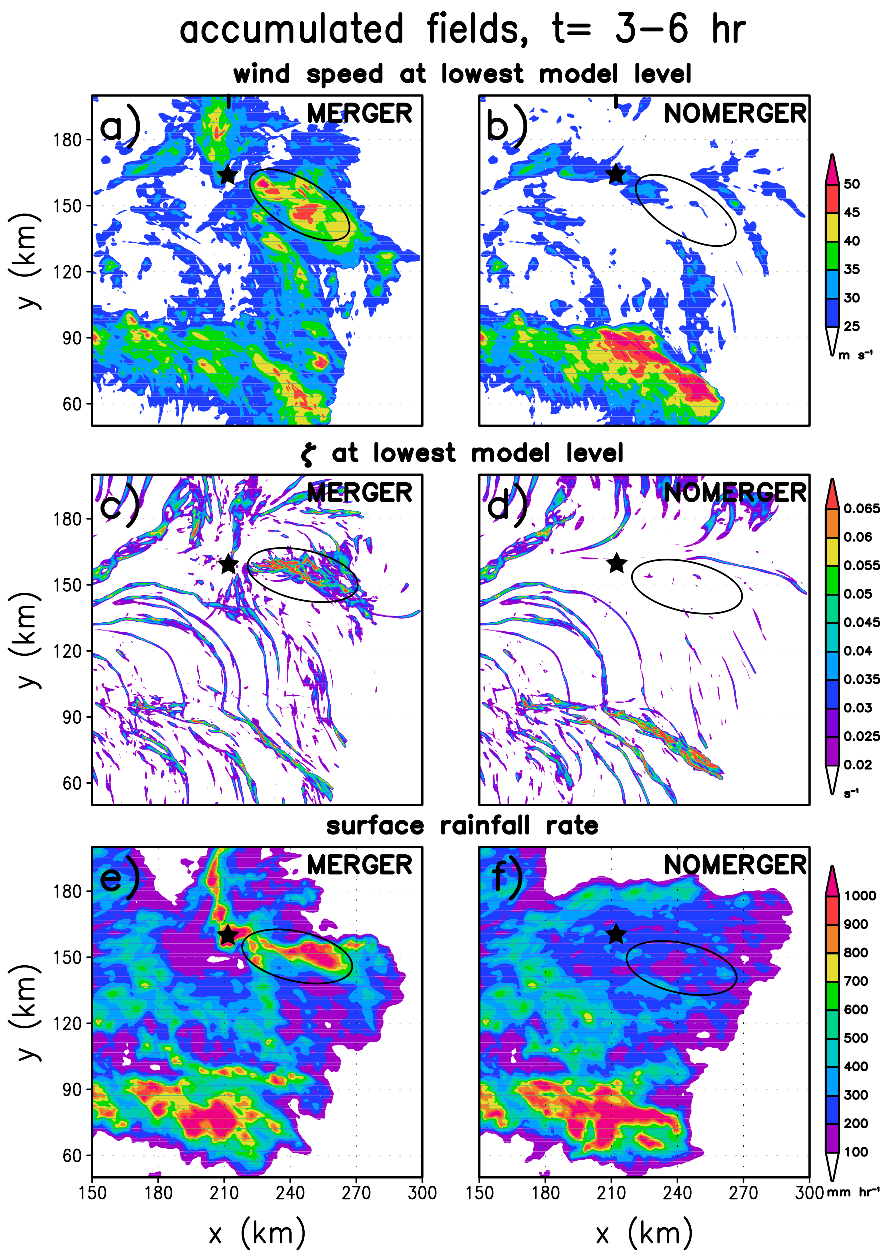

Figure 11: Swaths of maximum wind speed (top panels, m s^{-1}, shaded as shown) and vertical vorticity (middle panels, s^{-1}, shaded as shown) at the lowest model level, and rainfall rate (bottom panels, mm hr^{-1}, shaded as shown) accumulated between 3 and 6 hours into the simulation for the a, c, e MERGER and b, d, f NOMERGER simulations. The fields are accumulated by taking the maximum value over time across the subset of the model domain shown. Black start denotes approximate merger location, with ovals denoting areas where the merger produces substantial differences between the simulations.